



AIAA 2000-3514

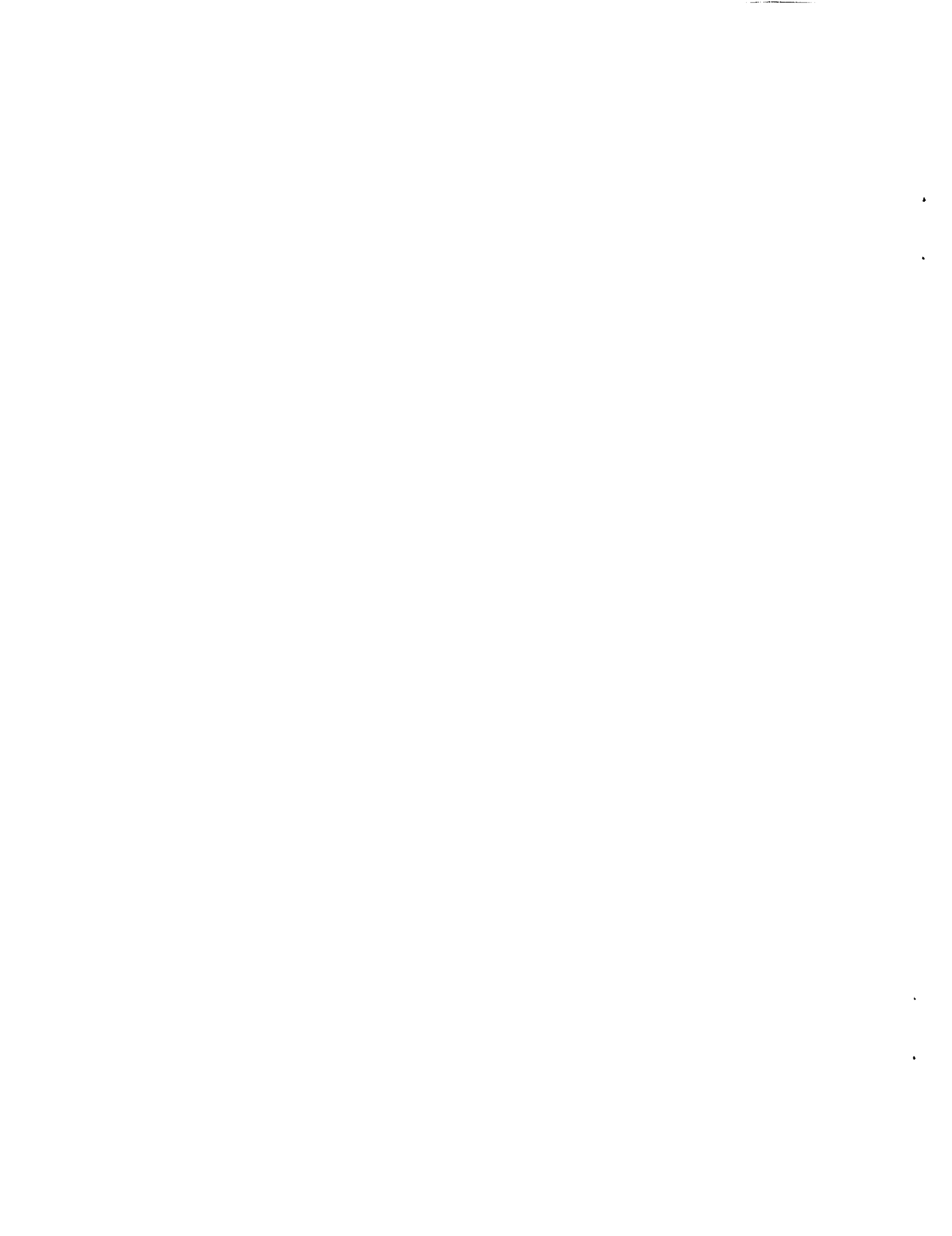
**WSTF Propulsion and Pyrotechnics
Corrective Action Test Program
Status—2000**

R. Saulsberry, J. Ramirez, H. L. Julien, M. Hart, and W. Smith
NASA Johnson Space Center
Las Cruces, New Mexico 88004

L. J. Bement
NASA Langley Research Center
Hampton, Virginia 23681-0001

N. E. Meagher
Texas Woman's University
Denton, Texas 76208

**36th AIAA/ASME/SAE/ASEE Joint
Propulsion Conference and Exhibit
July 17-19, 2000 / Huntsville, AL**



**WSTF PROPULSION AND PYROTECHNICS CORRECTIVE ACTION
TEST PROGRAM STATUS – 2000**

R. Saulsberry* and J. Ramirez†
NASA Johnson Space Center
White Sands Test Facility
Las Cruces, New Mexico

H. L. Julien,‡ M. Hart,§ and W. Smith§
Honeywell Technology Solutions Inc.
NASA Johnson Space Center
White Sands Test Facility
Las Cruces, New Mexico

L. Bement¶
NASA Langley Research Center
Hampton, VA

N. E. Meagher#
Texas Woman's University
Denton, TX 76208

ABSTRACT

Extensive propulsion and pyrotechnic testing has been in progress at the NASA Johnson Space Center White Sands Test Facility (WSTF) since 1995. This started with the Mars Observer Propulsion and Pyrotechnics Corrective Action Test Program (MOCATP). The MOCATP has concluded, but extensive pyrovalve testing and research and development has continued at WSTF. The capability to accurately analyze and measure pyrovalve combustion product blow-by, evaluate propellant explosions initiated by blow-by, and characterize pyrovalve operation continues to be used and improved.

This paper contains an overview of testing since MOCATP inception, but focuses on accomplishments since the status was last reported at the 35th Joint Propulsion Conference, June, 1999.¹ This new activity includes evaluation of 3/8-in. and -in. Conax pyrovalves; development and testing of advanced pyrovalve technologies; investigation of nondestructive evaluation techniques to inspect

pyrotechnically induced hydrazine explosions both through testing and modeling.

Data from this collection of projects are now being formatted into a pyrovalve applications and testing handbook and consensus standard to benefit pyrovalve users and spacecraft designers. The handbook is briefly described here and in more detail in a separate paper.²

To increase project benefit, pyrovalve manufacturers are encouraged to provide additional valves for testing and consideration, and feedback is encouraged in all aspects of the pyrotechnic projects.

INTRODUCTION

The Mars Observer (MO) failure review board identified propulsion and pyrotechnic systems issues as potentially contributing to the loss of the MO spacecraft. The board recommended review and generation of necessary test data, and publishing standards, alerts, and design guidelines to enhance NASA's spacecraft systems. In response, NASA Headquarters established a Mars Observer Propulsion and Pyrotechnics Corrective Action Test Program (MOCATP) with representatives from NASA Headquarters, White Sands Test Facility (WSTF), several NASA Centers, and industry. WSTF was requested to perform testing and help prepare documentation necessary to support the corrective action effort.

Because safety in future NASA programs is of concern, a rapid transfer of data from this program to other NASA and industry space programs is a major consideration. The evaluation of 3/8-in. Conax valves includes operational margin testing being accomplished at the NASA Langley Research Center (LaRC). To maximize program benefits, several status briefings were provided to release findings and provide opportunities for input from the propulsion community. The program was initiated by a

* Project Manager, NASA-WSTF Laboratories Office

† NASA Co-op Student, NASA-WSTF Laboratories Office.

‡ Science and Technology Lead, NASA-WSTF Laboratories Department

§ Project Leads, NASA-WSTF, Laboratories Department

¶ Pyrotechnic Engineer, NASA Langley Research Center

NASA Faculty Fellow

Copyright © 2000 by the American Institute of Aeronautics and Astronautics, Inc. No copyright is asserted in the United States under Title 17, US Code. The Government has a royalty-free license to exercise all rights under the copyright claimed herein for governmental purposes. All other rights are reserved by the copyright owner.

pyrovalves seals and make real-time measurement of housing deformation; and investigation of

meeting, August 23, 1995 at WSTF to form the test plan.³ As the test program continued, an extensive international review was provided at the WSTF Propulsion/Pyrotechnics Workshop IV in October 22 through 25, 1996. Additional findings were briefed on an annual basis at the 1996-1999 Joint Propulsion Conferences.^{1, 4 to 10} An in-depth description of testing up to 1999 is presented in "Mars Observer Propulsion and Pyrotechnic Corrective Actions Test Program Review-1999."¹

PROGRAM OVERVIEW

Primary MOCATP objectives included:

- Develop a process to accurately quantify pyrovalve combustion product blow-by, and then determine the maximum potential blow-by from various valves manufactured by OEA Aerospace, Inc. (previously know as Pyronetics Devices).
- Evaluate the potential for explosive thermal decomposition of hydrazine and monomethyl-hydrazine (MMH); determine the ignitability of MMH and nitrogen tetroxide (N₂O₄) resulting from pyrotechnic blow-by from high-fidelity reusable pyrovalve simulators (PVS). This was done to help experimentally validate or invalidate one of the MO boards failure scenarios and apply the test techniques to a wide variety of propulsion systems.
- Help establish corrective actions to protect and enhance future NASA spacecraft propulsion systems. This was to include evaluation of alternative pyrovalves and publishing standards, alerts, and design guidelines.

Follow-on funding was provided from agency sources to continue pyrovalve blow-by and operational margin testing, development of advanced pyrovalve sealing technologies, research of explosive decomposition of hydrazine, development of a chemical kinetics model for the explosive decomposition process, development of nondestructive (NDE) evaluation techniques for inspection of pyrovalves, and development of a pyrovalve testing and applications handbook and associated consensus standard.

APPROACH

The original program was organized to systematically investigate open MO issues to gain fundamental insight and then apply resulting corrective actions to future NASA spacecraft. The approach evolved to focus less on MO specifics and more on providing urgent support for near-term programs. The following summarizes the course currently being followed. Figure 1 illustrates the program flow with propellant interaction testing to the right of the start point and blow-by testing to the left of the start point.

A high-fidelity PVS simulating the OEA 1420-7 stainless steel (CRES) configuration was designed and fabricated at WSTF. The 1420-7 was first selected for use on the Advanced X-ray Astrophysics Facility (AXAF), and help was requested in verifying its safe operation. This unique configuration has side-mounted pressure cartridges with a built-in restriction between the cartridge and the ram. Ram velocity measurements were taken using VISAR.^{5,6} VISAR is a velocity interferometer which analyzes the Doppler shift in laser light with respect to time to make nonintrusive high-speed measurements.

The PVS blow-by was calibrated in the blow-by test system. The PVS was then installed in a hydrazine test system, and hydrazine thermal decomposition was evaluated under spacecraft-use conditions. An AXAF programmatic decision was then made to change to Conax valves with interference fit ram/sleeve assemblies; therefore, the amount of 1420-7 propellant testing was limited. A center-port head was then built to simulate the OEA CRES 1350-13 pyrovalve configuration used on the Landsat-6. The PVS blow-by was calibrated. This PVS was also tested in the hydrazine test system and differences in the two configurations were evaluated. During this testing, the PVS blow-by range that initiated thermal decomposition was explored. Most of the propellant interaction testing was done with the 1350-13 configuration because it did not have a restriction between the pressure cartridge and ram and was considered worst case.

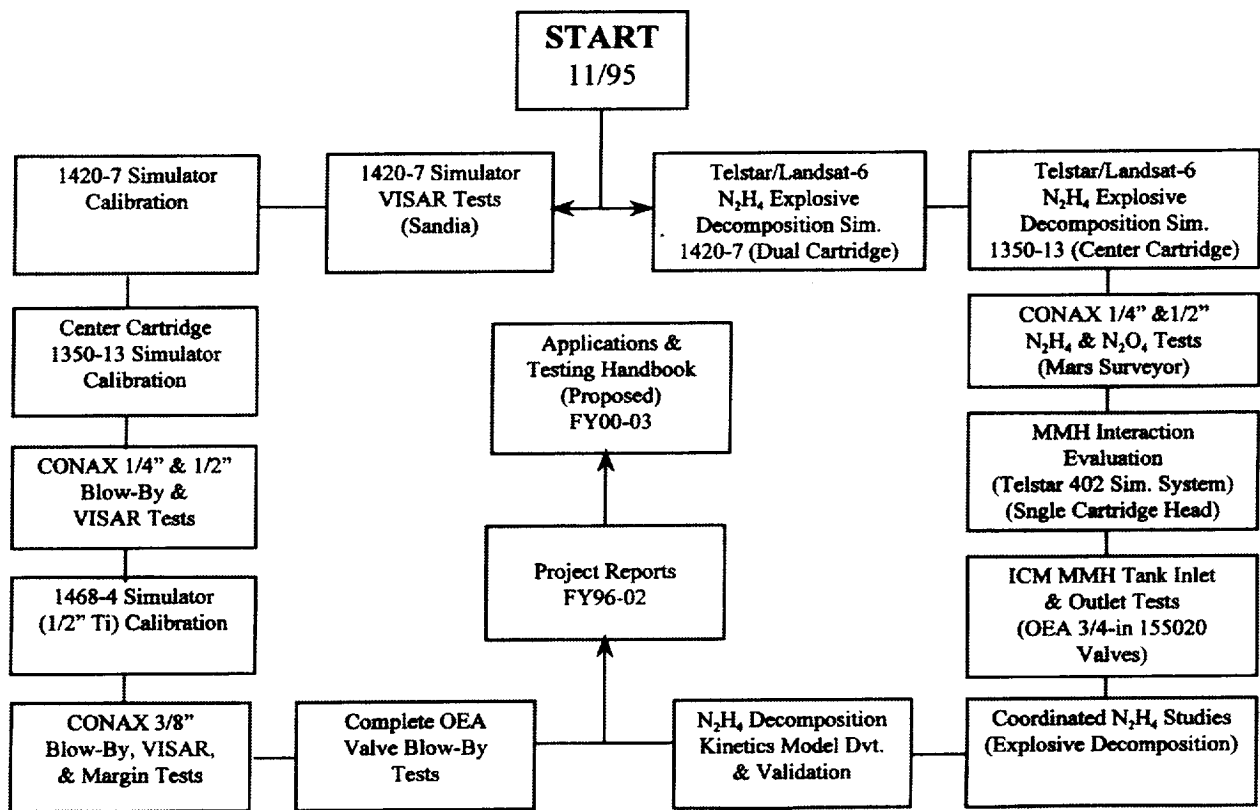


Figure 1. Mars Observer Propulsion and Pyrotechnics Corrective Action Test Program Flow Chart

At this point in the program, $\frac{1}{4}$ -in. and $\frac{1}{2}$ -in. Conax low blow-by pyrovalves became available for testing and were procured. The propulsion system community asked that the Conax valves be tested to support programs such as Mars Surveyor 98, which planned to use Conax valves. These valves were first tested in propellant to verify that explosive hydrazine decomposition would not occur during the near term Mars Surveyor 98 mission.

Following the Conax propellant testing, the hydrazine PVS testing was repeated in 1997-98 using MMH at the request of the International Space Station (ISS), Interim Control Module (ICM) Program. This was accomplished to compare the sensitivities of the two propellants to pyrovalve-initiated reactions. At the conclusion of this testing, the propellant interaction system was modified to closely simulate the pyrovalve interface to the ICM MMH tank inlet and outlet.⁸ This testing used ICM, OEA, 155020 flight-type pyrovalves.

A high-fidelity $\frac{1}{2}$ -in. titanium (Ti) 1468-4 PVS was also fabricated and calibrated in the blow-by test system. However, the planned propellant interaction testing using this simulator was deleted.

Additionally, blow-by from MO and various other configurations of OEA valves was to be evaluated.

Blow-by testing of two $\frac{1}{4}$ -in. and one $\frac{1}{2}$ -in. valves was also completed in 1998.⁹ Ten Conax $\frac{3}{8}$ -in. valves were also procured, and testing was initiated in fiscal year (FY) 1999. The test plan called for seven of the valves to undergo performance characterization at WSTF and three valves were to undergo operation margin testing at the LaRC. (As of July 5, 2000, six of the $\frac{3}{8}$ -in. valves had been tested at WSTF and two at LaRC.)

Making use of propulsion community inputs and data from testing, development of advanced pyrovalve technology was initiated in FY98 to help meet the need of future spacecraft. Design criteria suggested and explored include mass reductions, zero blow-by, zero particulate release, and lower pyro-shock. In FY98, new rams and cylinder configurations were designed and fabricated; testing of these designs in a specially designed PVS is continuing.

WSTF was also asked to develop NDE techniques to help reduce risk where pyrovalves with conventional O-ring seals are still used. Investigation of proposed technologies included

neutron radiography (NR), neutron computed tomography (NCT), conventional X-ray, X-ray computed tomography (XCT), reverse-geometry X-ray (RGX), and ultrasonic computed tomography (UCT). A summary of results from this effort is discussed in the Test Results Summary.

Related projects were also initiated to provide a foundational understanding of the physics and chemistry of the hydrazine explosion mechanism relevant to aerospace systems. In other energetic media it is known that the presence of voids, bubbles, cracks or other discontinuities can sensitize media to explosive initiation. This basic mechanism has been suspected of contributing to explosive events observed in spacecraft and simulations. Basic research in hydrazine chemical kinetics is also in progress to help create the tools necessary to model experimental test systems and analyze their results.

Ultimately, the data from the many associated projects is to be interpreted, associated, and formatted to form a pyrovalve testing and applications handbook.

TEST SYSTEM DESCRIPTIONS

This program makes use of WSTF hazardous fuel test facilities and the LaRC Pyrotechnic test laboratories. These extensive independent pyrovalve verification test capabilities are now available for NASA and industry programs. The discussed pyrovalve testing is performed in one of three locations, the WSTF Propellant Interaction Test Facility, the WSTF Blow-by/VISAR Analysis Laboratory, or the LaRC Pyrotechnic Test Facilities.

NASA WSTF Propellant Interaction Test Facility. This WSTF facility is capable of testing potential pyrotechnic interactions with most common rocket engine propellants, such as hydrazine, MMH, N_2O_4 , hydrogen, and oxygen. Additionally, propellants can be saturated with gases as required to simulate actual mission conditions. Most spacecraft propellant system configurations can also be simulated, and combined effects of hot pyrotechnic blow-by and adiabatic compressive heating can be evaluated. High-speed video, up to 12,000 frames-per-second can be used to track system fragmentation and help determine the speed of reactions.

Larger involvements of up to 500-lb TNT equivalents can be handled at WSTF's High Energy Blast Facility. This test area was used to investigate the effect that entrained gas bubbles have on liquid hydrazine detonation sensitivity.

NASA WSTF Blow-by/VISAR Analysis Laboratory. The Laboratory (Figure 2) has extensive capabilities. Valve pyrotechnic actuation and ram downstream pressures, temperatures, strain, light

emission, shock, blow-by gas and solid constituents, and ram velocity can be measured and analyzed. Prior to valve initiation, the system is evacuated to a target pressure of 10^{-7} Torr. Gas constituents are recorded before, during and after valve initiation using a Quadrupole Residual Gas Analyser (RGA). A gas chromatograph (GC) is also available. The GC originally handled gas analysis, but the RGA was added for greater sensitivity in support of Conax blow-by analysis.

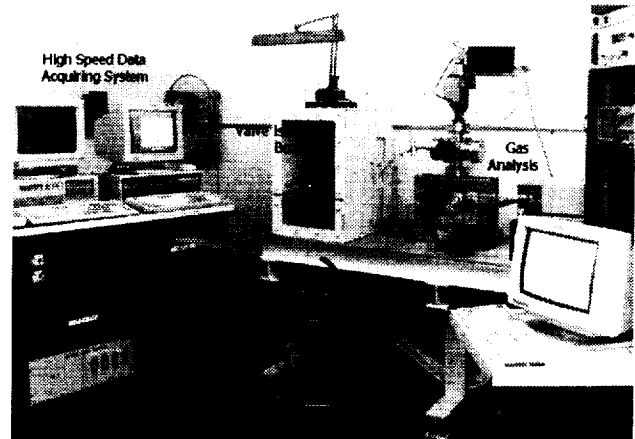


Figure 2. Blow-by/VISAR Analysis Laboratory

Any recorded gas from the initiation is analyzed for potential blow-by constituents, and assuming an ideal gas, the mass of the gaseous blow-by is determined. A fast ($1 \mu s$ rise time) sensitive vacuum transducer was added in 2000 and is configured to sense pressure as close to the tube shear section as possible in an attempt to measure pressure prior to any condensation of metal vapors. This transducer can detect very slight instantaneous pressure increases associated with very low blow-by valves.

Blow-by deposits are removed from the valve by a comprehensive ultra-pure water flushing process and then filtered at $0.2 \mu m$. The particulate can be counted, sized, and any unusual particles can be analyzed using a scanning electron microscope and X-ray electron dispersive analysis.

The particulate is digested and analyzed separately from the water-soluble portion using inductively coupled plasma mass spectroscopy (ICP-MS). Flush fluid is typically first analyzed for F and Cl by ion chromatography and then acidified and analyzed with the ICP-MS. Typically analysis is for Ti, Fe, Ni, Cr, Zr, K, and any added tracer chemicals (i.e., Gadolinium). However, specific analysis varies depending on the propellant used. Blow-by mass can be detected below $1 \mu g$. This sensitivity is available because both the RGA and

ICP-MS both have a parts per billion detection capability.

When ram velocity is measured simultaneously with blow-by measurements, a leak-tight optical window is installed. The VISAR can then track velocities from just a few meters/second to several hundred meters/second if required.

High-speed instrumentation and data acquisition systems are available to obtain a wide variety of dynamic and static measurements. Typical high speed measurements are sampled at rates of 1 MHz. Piezoelectric dynamic pressure transducers, such as PCB^{**}, are generally used for measuring higher frequency data. Piezoresistive units, such as Kulite^{**} probes, are also used. VISAR digitizing is handled at a 2 GHz sample rate.

NASA LaRC Pyrotechnic Test Facilities. These facilities have capabilities of high-performance functional evaluations, reliability predictions, environmental testing and non-destructive testing of a wide range of pyrotechnics (explosive and propellant-actuated mechanisms). Storage facilities, assembly and checkout bays and test bays, meeting military site standards, provide the capability to accommodate a variety of component and system level evaluations.

Unique test methods have been developed to determine functional margins of pyrotechnic mechanisms by measuring the energy required to function a device for comparison to the energy delivered by the pyrotechnic energy source. *Energy Required* is determined by dropping weights on the actuating mechanism of a device. This simulates the impulsive input from a pyrotechnic energy source. The *Energy Delivered* is determined by measuring the work output of the moving portion of the mechanism. For example, the velocity of a piston in a valve at the point of actuation provides kinetic energy, $1/2 mv^2$. High-response piezoelectric transducers measure pressure and forces during functional evaluation. These data can be further analyzed to determine statistical functional margins with as few as 5 final demonstration units. A test apparatus is available to determine the amount of gaseous blow-by around an activating piston, and to determine the constituents of the gas. Also available are electrical inspection instruments, firing systems, and electrostatic discharge.

Environmental simulations, such as vibration, shock, and thermal vacuum provide a capability to conduct qualifications for spacecraft pyrotechnics. The vibration systems have the capability of 10,000 force-pounds and accelerations of several-

hundred g's in all axes; slip tables expand the amount of mass that can be tested. The thermal/vacuum chambers have internal dimension of 5 feet in diameter, vacuum levels to 10^{-7} Torr, and solar heat simulation and cryogenic shrouds.

RESULTS SUMMARY

The MOCATP and follow-on test programs followed the flow chart in Figure 1. The results obtained in each branch are described in this section.

Blow-by and VISAR Testing

Over 50 blow-by tests have been performed to date. All tests performed prior to FY00 are described in the previous AIAA status paper.¹ However, only Conax valves were tested in FY00 and, for completeness, all the low blow-by Conax valves are summarized in Table I of the current paper.

Sandia VISAR Tests. Following development of the CRES 1420-7 PVS, VISAR testing was first accomplished. This verified that the PVS would function in a similar manner with or without O-rings installed. This was important because the PVS was to be fired without O-rings during many of the propellant interaction tests to simulate the worst-case scenario of O-ring failure.⁵

1420-7 PVS Calibration. Following Sandia VISAR tests, the 1420-7 CRES PVS was calibrated in a newly constructed blow-by test system at WSTF.

**PCB Is a registered trademark of Piezotronics Inc., Depew, NY

** Kulite Is a registered trademark of Tungsten Corp. East Rutherford, NJ

ID CO- TST-	Date	Size	Booster (mg) [§]	Blow-by	Ram Velocity (m/s)
01	08/97	_ in.	100	No pressure rise measured (initial evacuated). Blow-by deposits: 0.096 mg water soluble metal salts and 0.064 mg of insoluble particulate	105
02	08/97	_ in.	120	Pressure rise of 100.1 Torr from trapped air below ram. Blow-by deposits: 0.042 mg of water soluble metal salts and 0.060 mg of insoluble particulate	N/A
03	09/97	_ in.	100	Pressure rise of 25.0 Torr from trapped air below ram. Blow-by deposits: 0.054 mg of water soluble metal salts and 0.050 mg of insoluble particulate.	N/A
04	08/98	_ in.	100	No pressure rise measured (initially evacuated). Blow-by deposits: 0.026 mg of water soluble metal salts and 0.050 mg of insoluble particulate.	Lost signal
05	06/00	-in.	120	Pressure spike of 100 Torr below ram. [¶] Gaseous blow-by constituents indicated by the RGA. [§] Deposits: 0.009 mg water soluble metal salts and 0.007 mg of insoluble particulate.	N/A
06	05/99	3/8-in.	200	No pressure rise measured below the ram. Deposits: 0.0128 mg of water soluble metal salts and 0.0123 mg of insoluble particulate.	97
07	05/99	3/8-in.	200	No pressure rise measured. Deposits: 0.037 mg of water soluble metal salts and 0.009 mg of insoluble particulate	106
08	06/99	3/8-in.	200	Anomaly of non-flight booster	N/A
09	08/99	3/8-in.	200	No pressure measured rise below the ram. RGA did not show significant gases above the S/N ratio.	> 85
10	05/00	3/8-in.	200	Pressure spike of 38 Torr below ram. [¶] RGA indicated gaseous blow-by of pyrotechnic constituents (Fig. 4). [§] Blow-by deposits: 0.027 mg water soluble metal salts and 0.009 mg of insoluble metal salts.	N/A
11	06/00	3/8-in.	200	Pressure spike of 112 Torr below ram. [¶] (Fig. 3). RGA indicated gaseous blow-by of pyrotechnic constituents. [§] Blow-by deposits: 0.049 mg water soluble metal salts and 0.003 mg of insoluble particulate.	N/A
12	Planned	-in.	120		

[¶]New high response, high sensitivity pressure transducer added (began in FY00). Previously used only a low response vacuum transducer that did not register pressure spikes (approx. 0.05 Torr steady state resolution.)
[§] Non-quantitative method to observe very minute evidence of gaseous blow-by using the RGA.
[§] Two NASA Standard Initiators used to ignite booster.

Table 1. Conax Pyrovalve Test Matrix

However, the process has been continuously improved and updated. Twelve successful calibration points were obtained over a clearance range of 0.00215 to 0.00725 in. Associated blow-by ranged from 0.92 to 32.37 mg.² 1350-13 Simulator Calibration. During hydrazine interaction testing, a single-center-initiator head was fabricated simulating the OEA 1350-13 configuration. The associated blow-by calibration provided additional insights into comparative operations characteristics. Additionally, the Pressure and Ram Velocity Affect on Blow-by was noted. The dual port valve had notably higher blow-by than the single-port curve, even though the single-port pressures were higher.

1468-7 Simulator and Flight Valve Testing.

Four Ti 1468-7 PVS tests and three flight valve tests were accomplished. The PVS tests are identified as HB-TST13-17 and the flight valve tests are identified as MO-TST01-03 in Table 1. Both the PVS and flight valves appeared to have very similar operational characteristics as verified by both blow-by and VISAR testing. These valves were also noted as overpowered, developing largely amounts of Ti fragments and particulate that formed during the valve operation. If the fragments were discarded, blow-by was relatively consistent with CRES 1350-13 valves.

Conax Blow-by Testing. The evaluation of Conax valves as a possible corrective action involved both propellant testing and blow-by/VISAR testing.

Data from the Conax blow-by testing are shown in Tables 1 to 3.

The manufacturer expected that the valves had essentially zero blow-by and the configuration of the valve made the expectation appear reasonable. Although slight blow-by appears to consistently occur, the blow-by has been confirmed to be very low on the eleven valves tested to date.

The first $\frac{1}{2}$ -in. valve to be tested was modified for VISAR, involving the installation of a sealed window over a small port in the valve opposite the ram. The window and VISAR tracked the velocity of the shear cap effectively and reached a maximum of 105 m/s.

The VISAR window adapter also contained a capillary tube, which was tied back into the blow-by system allowing evacuation of the air. Although traces of pyrotechnic products of combustion and particulate from the shear operation were found in the flush water no measurable pressure rise was noted following valve actuation. Vacuum pressure resolution was excellent at approx. 0.1 Torr, but the transducer response was too slow to see a pressure rise before the vapors deposited out. (In later tests, a high response vacuum pressure transducer was located near the lower part of the valve and the short term pressure increase was noted.) Referring to Table 1, CO-TST01, a total of 0.096 mg of water soluble metal salts was found in the flush fluid. In addition, another 0.064 mg of insoluble metal particulate, likely from the shear operation, was noted.

A $\frac{1}{2}$ -in. valve and a second $\frac{1}{2}$ -in. valve was then tested. These valves were not modified and were connected only at the fluid interface lines. The water flush of the $\frac{1}{2}$ -in. valve accumulated a total of 0.042 mg of soluble metal salts and 0.060 mg of insoluble metal particulate. The same flush applied to the second $\frac{1}{2}$ -in. accumulated a total of 0.054 mg of soluble metal salts valve and 0.050 mg of insoluble metal particulate as shown in Table 1, CO-TST03.

A third Conax $\frac{1}{2}$ -in. valve was tested in July 1998. This valve was also modified to obtain VISAR data. This valve had the same general order of magnitude blow-by shown in Table 1, CO-TST04. However, water soluble deposits were somewhat less at 0.0262 mg. The particulate generated by the shear operation was very consistent at 0.050 mg. A maximum velocity was not obtained on this test because the shear cap being tracked apparently cocked

or rotated slightly during travel, and the laser signal was lost after reaching approximately 45 m/s.

Ten $\frac{3}{8}$ -in. valves were also procured in December 1997, but testing did not start until 1999. Two of the valves were tested by June 1999 and are identified as CO-TST06 and CO-TST07 in Table 1. Test system modifications were first made in an effort to optimize sensitivity as described in the Test System Description section.

Both $\frac{3}{8}$ -in. valves were modified to add a VISAR window and the velocity of the shear cap was measured. The maximum obtained velocity of 97 m/s was noted on the first test and the shear cap reached 106 m/s on the second test.

Blow-by and particulate data from the $\frac{3}{8}$ -in. valves were generally lowest of the Conax valves tested to date. From Table 1, test CO-TST06, we see that 0.0162 mg of water-soluble deposits and 0.0123 mg of particulate were flushed from the first $\frac{3}{8}$ -in. valve. The second $\frac{3}{8}$ -in. valve tested yielded 0.03612 mg of water soluble deposits and 0.000846 mg of particulate.

In FY00 the fast, sensitive vacuum transducer, was installed in the test system. The new sensor has been used for three tests thus far; two $\frac{3}{8}$ in. (CO-TST10 and CO-TST11) and one $\frac{1}{2}$ in. (CO-TST05) Conax pyrovalves. Each test has indicated an appreciable yet narrow pressure spike for each valve tested; 38 Torr on TST10, 112 Torr on TST11, and 100 Torr on TST05 (Figure 3). For each of these tests, simultaneous pressure rises were not seen on the slow conventional sensors that the program

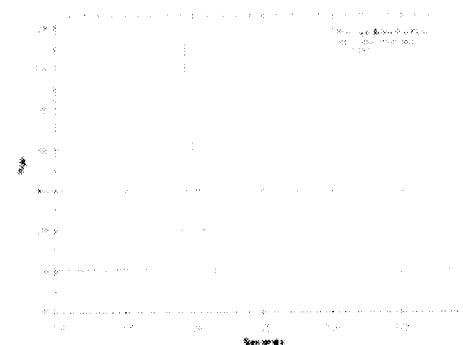


Figure 3. High Response Vacuum Transducer Pressure Trace (located below the ram, near the shear-cap interface).

Table 2. Conax Blow-by Insoluble Particulate Data

Test	Water Insoluble Particulate (mg)					
	Ni	Fe	Zr	Cr	Ti	K

CO-TST01, _-in.	ND	0.012	ND	0.047	ND	0.0051
CO-TST02, _-in.	ND	0.0025	ND	0.048	ND	0.0093
CO-TST03, _-in.	ND	ND	ND	0.044	ND	0.0054
CO-TST04, _-in.	0.0065	0.040	ND	ND	0.0035	ND
CO-TST05, ½-in.	ND	ND	ND	0.0007	ND	ND
CO-TST06, ⅜-in.	0.0021	0.0033	ND	0.0017	0.0052	ND
CO-TST07, ⅜-in.	0.0005	0.0058	ND	0.0012	0.0009	ND
CO-TST10, ⅜-in.	0.0015	0.0039	ND	0.0033	0.0002	ND
CO-TST11, ⅜-in.	0.0003	ND	ND	0.001	ND	0.0015

NOTES: ND = None detected above reporting limit.

Table 3. Conax Blow-by Soluble Deposit Data

Test	Water Soluble Blow-by (mg)							
	Ti	Zr	K	Fe	Cr	Ni	Cl ⁻	F ⁻
CO-TST01, _-in.	ND	ND	0.068	ND	ND	0.010	0.015	0.0025
CO-TST02, _-in.	ND	ND	0.028	ND	ND	ND	0.0112	0.0026
CO-TST03, _-in.	0.021	ND	0.028	ND	ND	ND	0.0052	ND
CO-TST04, _-in.	ND	ND	0.0021	ND	0.0012	0.0019	0.021	ND
CO-TST05, ½-in.	ND	ND	ND	ND	0.0086	0.0003	ND	ND
CO-TST06, ⅜-in.	ND	ND	0.0019	ND	.00127	0.0002	0.0062	0.0032
CO-TST07, ⅜-in.	0.0008	ND	0.0078	0.0120	0.0014	0.0018	0.0088	0.0043
CO-TST10, ⅜-in.	ND	ND	ND	0.0193	0.0067	0.0007	ND	ND
CO-TST11, ⅜-in.	ND	ND	ND	0.011	0.0363	0.0015	ND	ND

NOTES: ND = Not detected above reporting limit

previously relied upon. The additional pressure in the system is only temporary since approximately 95 percent of the metal vapor quickly deposits out. According to chemical equilibrium calculations performed for the pyrotechnic charges with an available computer code. As can be seen from Table 1, these valves had blow-by deposit mass that was similar to previous valves. A detailed breakdown of constituents in deposits and particulate is listed in Tables 2 and 3. Because of the difficulty of quickly acquiring and analyzing blow-by gasses, data was gathered using an approach that differed from the previous methods for these three recent tests. In these tests, the blow-by gas was not contained and then later sampled as in the past, but was allowed to immediately flow through a capillary tube directly to the RGA/high vacuum sampling system. This allowed the slight *puff* of blow-by gas to be analyzed within seconds of generation. This method requires the pyrovalves to be completely evacuated to the same high vacuum level as the RGA system. Although rigorous quantitative analysis is not easily done using this method, a credible amount of expected blow-by constituents from the initiators was seen for the first time from Conax pyrovalves (Figure 4). Work is currently being done to perfect the method and quantify the amounts of gasses analyzed.

Functional Evaluation of Conax Pyrovalves

The operational characteristics of normally-closed Conax pyrovalves are being evaluated at LaRC. The goal of this effort is to determine the functional margin of this valve by determining the energy required to function the valve for comparison to the energy delivered by the booster charge.^{12,13} The approach was to measure the *energy required* by conducting weight drop tests, and to measure the *energy delivered* by firing the pyrovalve cartridge assembly into a valve simulator (Future Testing and Modeling)

Weight drop tests. Figure 5 shows the experimental setup being used to determine the force and displacement versus time and the energy required to function the pyrovalve. The falling weight simulates the dynamic stimulus output of the valve's booster charge to drive the valve's internal piston to operate the valve. The velocity of the falling weight can be varied by changing the height from which the weight is dropped. The input energy to the valve can be varied by changing the drop height, the mass of

the drop weight, or both. When the weight contacts the actuating pin, it also begins to block the laser beam. A photocell detector, calibrated to the amount of light blocked, provides a direct readout of the position of the weight (Figure 6) and, consequently, the amount of stroke of the actuating pin against the valve's internal piston. A piezoelectric load cell underneath the assembly records the dynamic forces created throughout the stroke.

This test approach has been applied to a 3/8-in. Conax pyrovalve (interference fit ram). Test data indicates that surprisingly little energy is consumed in the stroking of the interference fit ram. Virtually all of the input energy was consumed in shearing out the fitting in the internal tube. This is indicated by the large peak reaching a force of 5,900 pounds and having a duration of approximately 0.35 milliseconds, (Figure 6).

Pyrovalve Nondestructive Evaluation. Prior NDE results¹ have shown that conventional X-ray and Reverse Geometry X-ray images do not have the ability to resolve O-rings within the ram grooves in either Ti or corrosion resistant stainless steel CRES pyrovalves. This is graphically illustrated in Figure 7a that is an X-ray radiograph through the more neutron-transparent Ti body. Additionally, an X-ray computed tomography (XCT) scan (not shown in Figure 7) of a 1/2-in. Ti body pyrovalve using the Sandia National Laboratories CT apparatus has proved able to resolve only a very faint shadow of an O-ring, so the extremely weak image was not useful in detection of O-ring damage.

In contrast, conventional N-rays radiography has shown (Figure 7b) excellent capability for imaging O-rings through Ti Pyrovalves when resolution is defined by a collimator length-to-diameter (L/D) ratio greater than 150. N-ray computed tomography (NCT) has also indicated outstanding capability (Figure 7c), but the cost of the NCT process was about an order of magnitude more than the conventional radiographs. Also, several valves may be imaged simultaneously using a single conventional radiograph, whereas NCT is generally applicable to a single test article at a time.

Conventional N-ray Defect Detection Limits.

Conventional neutron radiographs were used to explore defect-detection limits for pyrovalves made from both Ti and CRES. Ti and CRES OEA PVS

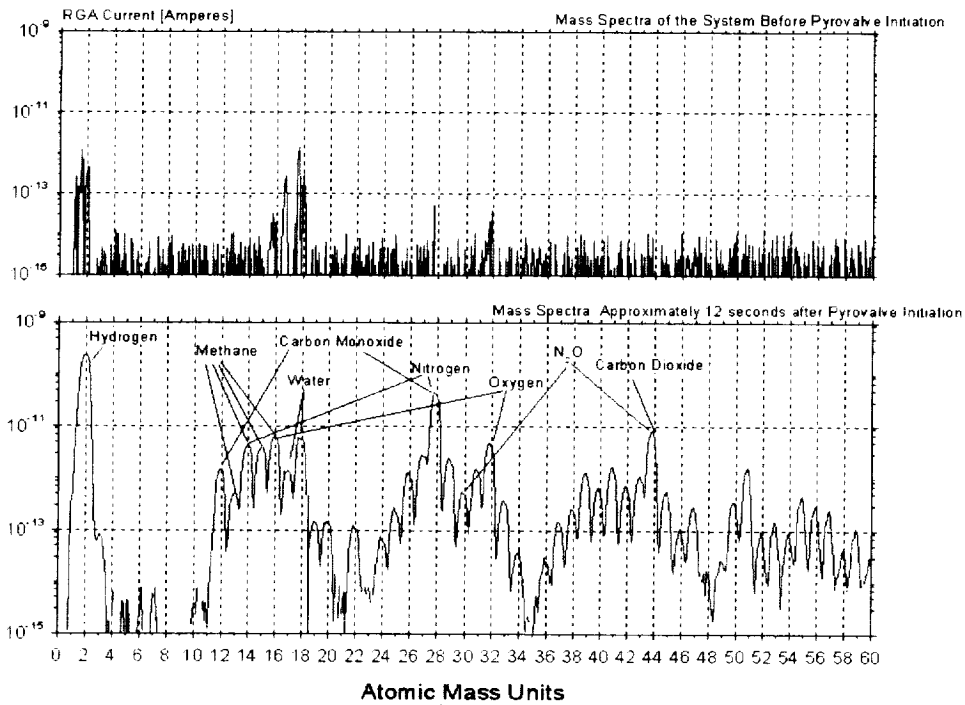


Figure 4. Mass Spectra of Blow-by from a 3/8 in. Conax Pyrovalve. (The peaks of various constituents are noted.)

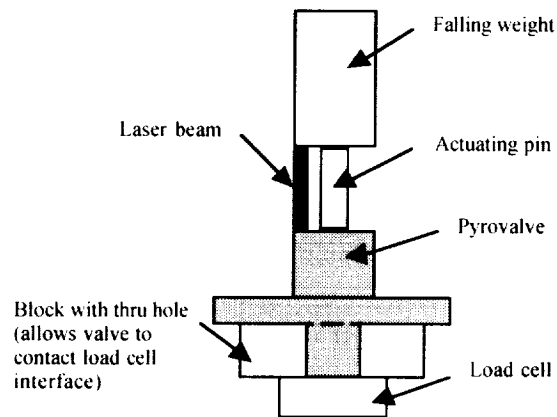


Figure 5. Simplified test setup to determine force and stroke versus time and energy required to actuate the pyrovalve.

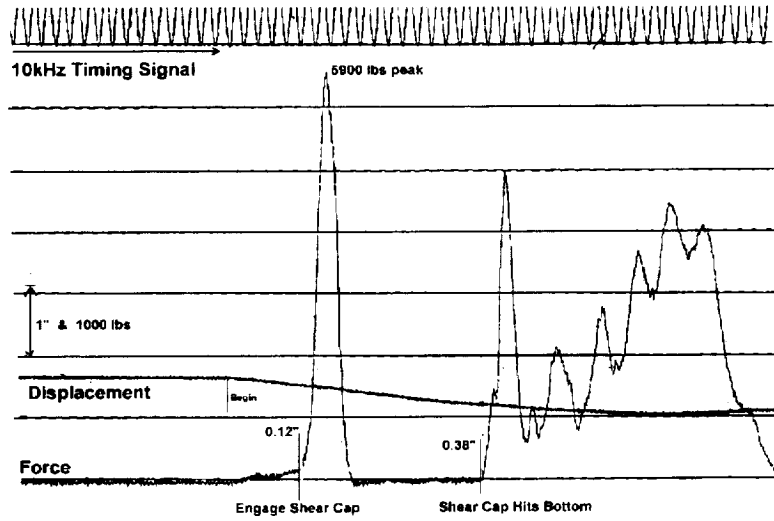
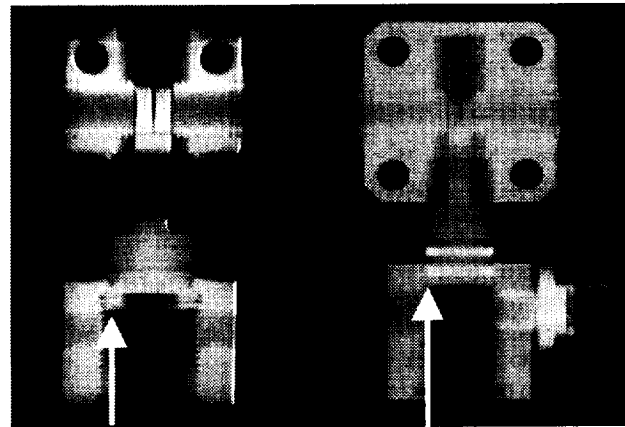
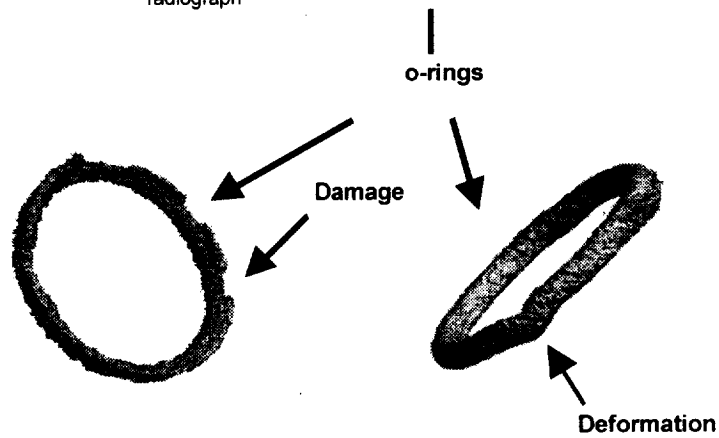


Figure 6. Weight Drop test of 3/8-in Conax Pyrovalve.



(a) Low density o-rings are not visible in X-ray radiograph

(b) O-rings visible in N-ray



Neutron-computed tomographs of top (left) and bottom (right) O-rings deformed and damaged during installation in Ti-body pyrovalve

Figure 7. Comparison of X-ray Imaging and Neutron Imaging of Pyrovalves with Installed O-rings

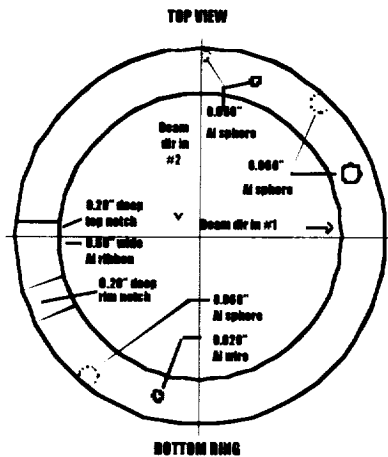


Figure 8. Location of Aluminum Inserts Used to Simulate O-ring Damage

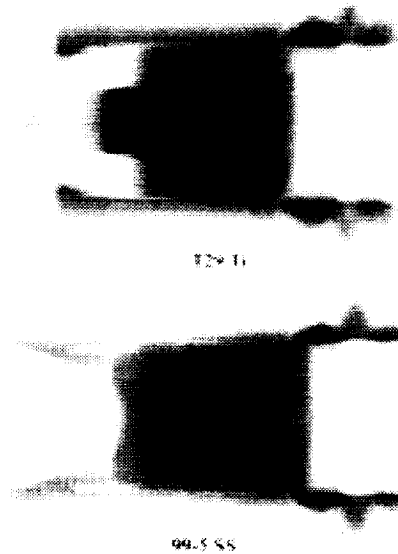
sleeve/ram assemblies were used as test articles and the ram O-rings were inflicted with known defects. The wall thickness of the PVS sleeves was designed to mimic that of the 1/2-in. pyrovalves.

The simulated O-ring defects were formed by inserting miniature aluminum spheres, aluminum wire segments, and aluminum ribbon segments into small holes drilled into the O-rings at prescribed positions. Two sizes of spheres, one 0.060-in. diameter and another 0.030-in. diameter, were installed at strategic locations in the O-ring. The wire and ribbon segments, each 0.020-inch thick, were installed at strategic locations in the quadrant diametrically opposite the spheres. The location of the inserts in the bottom O-ring is shown in Figure 8. An identical pattern was used for the top O-ring, except the pattern was rotated 90 degrees relative to that of the bottom ring. The purpose of the aluminum inserts was to accurately constrain the size of the drilled holes despite tension or compression of the O-rings by installation.

Otherwise, the aluminum inserts appeared on the neutron radiographs as accurately-defined near voids. All the radiographs of these simulators were performed with a neutron-beam collimator L/D ratio of approximately 284, so resolution was excellent.

For the O-rings on the Ti rams, both wire and sphere defects were easily discernable both in the flat view and in the tilted view. For these radiographs, the tilt angle was selected as approximately 20 degrees, rather than the 30 degrees used for the assembled pyrovalves. Both sizes of sphere defects (0.060 and 0.030in.) were readily identified, as

Figure 9. Comparison of O-ring Defect Detection through Ti and CRES Sleeves



was the 0.020-in. wire. The rim notch was more difficult to identify, and the top notch was essentially invisible. In contrast, for the O-rings on the CRES rams, only the larger spheres were weakly resolved in both the views, and that only in the film exposed to a 3.37 density (Figure 9).

Leak Path Detection. Conventional neutron radiographs were also made of Conax PVS sleeve/ram assemblies that use metal-to-metal seals rather than O-ring seals. These PVS assemblies had bodies fabricated from CRES. The wall thickness of the simulator sleeves was designed to mimic those of Conax 1/2-in. pyrovalves. Two of the PVS assemblies, identified as C1 and C2, were fitted with rams that duplicate the Conax specifications, and two of the PVS assemblies, identified as R1 and R2, were fitted with rams incorporating some WSTF modifications. Neutron radiographs of these four PVS assemblies had not been delivered. These results will be reported at the next JPC along with results of future testing.

The potential for using contrast agents (briefly called tracers) in valves to allow post-firing neutron radiographic imaging of leak paths was also investigated. The two forms of tracers planned for use were tetraboron carbide B_4C and gadolinium nitrate hexahydrate $Gd(NO_3)_3 \cdot 6H_2O$. The B_4C was in the form of an ultra-fine (approx. 1200 mesh) ceramic powder, and the $Gd(NO_3)_3 \cdot 6H_2O$ was dissolved in methyl alcohol at a concentration of 0.5 g/ml. A small quantity, about 0.25 g, of one or the other of these tracers was inserted on top of a pyrovalve ram prior to its actuation.

Tests to date have all used $Gd(NO_3)_3$ tracer and Ti-body OEA simulators. The technique was first applied to a firing incorporating T-17. This

configuration used tracer on a ram with pristine O-rings. A second and a third assembly, T-1 and T-28, both included tracer on a ram with no O-rings. Finally, a fourth assembly, T-22, included tracer on a ram with intentionally damaged O-rings. Neutron radiographs of these four tracer configurations had not been delivered. Finally, one Conax-type PVS, made of CRES at WSTF, was patterned after the corresponding provalve, but constructed without a taper in the cylinder bore.

The radiograph of T-17 showed copious tracer transferred to the top surfaces of the top O-ring. Note that the top O-ring was that nearest to the pyrotechnic chamber. All tracer visible in this radiograph has been contained by the top O-ring. In fact, the top O-ring was forced to the bottom of its groove, but the bottom O-ring remained at the top of its groove. No booster charge was used with these shots, so the overpressure in the pyrotechnic chamber was obviously appreciably lower than in a typical firing. Radiographs of typical firings with pristine pyrovalves show both O-rings forced to the bottom of their grooves.

The radiograph of T-13 showed that significant tracer material had leaked past the damaged top O-ring and accumulated on the top surface of the damaged bottom O-ring. All the tracer visible in this radiograph was, however, contained by the bottom O-ring, even though it was also damaged. Apparently because of the leakage past the damaged O-rings, neither of these O-rings were forced to the bottom of their respective grooves. The damaged area on the bottom O-ring was observed to have rolled during installation to the bottom surface of the ring, so apparently that ring sealed sufficiently to prevent tracer leakage. Leakage around the top O-ring was observed along the groove as well as along the cylinder wall.

The radiograph of the CRES PVS built at WSTF showed that tracer had leaked around both seals and had accumulated between the seals and at the base of the ram piston at its stop. Recall that this type of PVS has two metal-to-metal seals, rather than O-ring softgoods, as in OEA simulators.

N-ray Survey of WSTF Pyrovalve O-rings.

Conventional neutron radiographs were made of most of the pyrovalves held within the present WSTF inventory. This was done to screen for major defects and to allow planning of further NDE testing of these valves. The inventory included both those made of Ti and CRES. They included some in as-assembled unfired condition and a few in post-actuated condition. The inventory comprised OEA pyrovalves of several sizes ranging from $\frac{1}{2}$ -in. to $\frac{3}{4}$ -in. These radiographs were performed both with the pyrovalve bodies in a flat orientation and in a tilted

orientation. For the purpose of this discussion, a flat orientation is that for which the plane formed by the axis of the flow-pipe and the axis of the ram-cylinder is oriented perpendicular to the neutron beam. Correspondingly, the tilted orientation is that for which the pipe/ram plane is tilted about 30 degrees to the beam.

All these radiographs were performed with a neutron-beam collimator L/D ratio of approximately 250, so resolution was near optimal. Nevertheless, none of the pyrovalve radiographs in this group revealed major O-ring damage except those in which damage had been intentionally inflicted during disassembly. The resolution was, however, sufficient to identify slight non-uniformity in the O-ring cross section of a few of the installed O-rings. Among the radiographs of twenty-four pyrovalves with two O-rings in each (48 total rings), such non-uniformity was observed in only five O-rings. These pyrovalves are yet to be disassembled to determine the cause of the non-uniformity.

It should be noted that currently demonstrated defect-detection capability for CRES valves is limited. The current technique appears adequate for the $\frac{1}{2}$ -in. CRES valves since the valve body cylinder walls are thin enough to permit good O-ring contrast. However, the thicker cylinder walls of the $\frac{3}{4}$ -in. valves currently causes poorer O-ring contrast, pointing to the need for more process development. Additionally, several instances of significant O-ring damage has been noted on other flight qualified valves made of both Ti and CRES previously tested at WSTF, confirming the need for this type of NDE.

Propellant Interaction Testing

Propellant interaction test flow is shown to the right of START in Figure 1. The previous AIAA status paper discusses all previous interaction testing.¹ The Telstar 402/Landsat-6, $\frac{1}{2}$ -in. and $\frac{3}{4}$ -in. Conax, MMH, ICM, and Hydrazine Sensitivity testing tests was completed last year and the Mixed Phase Hydrazine testing and kinetic modeling remains in progress.

Telstar/Landsat-6 Simulations. The Telstar 402 activation scenario was chosen as the first test series to be performed. Both Telstar 402 and Landsat-6 flight anomalies are thought to have resulted from energetic hydrazine reactions that were initiated by a pyrovalve. The Telstar 402 test system configuration and test procedures were coordinated with LM to ensure test conditions and procedures used would be representative of LM ground testing. This testing utilized PVS that simulated both the $\frac{1}{2}$ -in. OEA CRES 1420-7 configuration and the $\frac{3}{4}$ -in. CRES 1350-13. This testing demonstrated system level

hydrazine reactions ranging from a relatively minor pressure rise to massive system destruction and fragmentation.¹

Conax Valve Testing. Conax $\frac{1}{2}$ -in. (1832-2024) and $\frac{1}{4}$ -in. (1832-204-1) valves were tested at the request of the Mars Surveyor 98 program. Two $\frac{1}{2}$ -in. and 3 $\frac{1}{4}$ -in. valves from the Mars Surveyor 98 lot were used for propellant interaction testing. The Conax tests were accomplished in the Telstar/Landsat simulation system to verify hydrazine reaction would not occur under the same conditions previously tested.

MMH Reactivity Test. The Telstar 402/Landsat 6 simulations previously performed using the 1350-13 PVS and hydrazine were repeated using MMH. The first two tests in this series were repeated at ram-to-bore clearances that had previously produced explosions with hydrazine, but no reaction was noted with MMH. The simulation was repeated a third time using a much larger clearance. This worst-case test again produced no reaction.³

ICM Outlet and Inlet Configuration Tests. After determining that MMH was much less reactive to blow-by than hydrazine, another test series was accomplished to determine if the unique ICM configurations and activation scenarios were safe. This test series consisted of one MMH tank outlet configuration test and two MMH tank inlet configuration tests. As with other MMH testing, no propellant reactions were noted. A detailed discussion of data is provided in a previous paper.⁸

Multiphase Detonation Testing. The possibility for a low velocity detonation in hydrazine media is also being studied. The pattern of damage observed in Telstar 402/Landsat 6 testing indicated an explosion mechanism capable of traveling along a considerable length of liquid fuel-laden stainless steel line that was neither a gaseous detonation nor a liquid phase detonation. This suggests that either a low-velocity detonation mechanism or some other complex mechanism was involved. To study this possibility, elements of the test system conditions under which the event was thought to have occurred are being duplicated. Initial testing to date has induced rapid hydrazine decomposition and subsequent failure of a stainless steel fuel line at a single point. Additional analysis and testing required to determine if propagation occurred is currently underway. Once the event is demonstrated to be repeatable, additional experiments can be conducted to parametrically analyze the process.

Homogeneous Phase Studies. Hydrazine vapor detonations also are being studied. The effect of diluents, common in hydrazine systems, on the vapor detonation process is being determined.¹⁴ Diluent concentrations required to prevent detonation of the

hydrazine vapor were determined, and a relative ranking of the effectiveness of the diluents was correlated to the ratio of specific heats (γ).

Condensed phase research also is in progress. The shock Hugoniot of liquid¹⁵ is being experimentally determined using an impedance matching technique in the pressure range of 3.1 to 21.4 GPa. This work developed basic equations of state data for liquid hydrazine at shock pressures.

Basic research in the area of thermodynamic modeling also is in progress. Soave-Redlich-Kwong (SRK) and Peng-Robinson (PR) equation of states (EOS) were developed and tested using a fugacity coefficient comparison method.^{16, 17} Basic hydrazine property data including critical properties, vapor pressure data, and heat capacity data were found to be self consistent. Based on the Peng-Robinson EOS, hydrazine thermodynamic properties were calculated and an enthalpy-pressure Mollier chart has been completed for hydrazine.

Chemical Kinetics Modeling. Finally, hydrazine kinetics are being studied in great detail. The ultimate objective of this work is to predict hydrazine decomposition. When combined with thermodynamic information and system-specific information, it will be possible to predict system temperatures and pressures as a function of time and ultimately predict the behavior of the system.

Current efforts address the anomalous behavior of liquid hydrazine observed in pyrovalve/fuel system testing at WSTF¹ that is likely to be initiated by gas-phase reactions between fuel vapors and blow-by species. In order to approach a problem of this complexity, it was considered preferable to start with the development of a detailed model of a simpler chemical system, the thermal decomposition of hydrazine. Expansion of the model, as necessary, to include the species introduced by the pyrovalves could then follow. As a result, the first goal of the modeling project was to develop and validate a detailed chemical-kinetic mechanism for the decomposition of hydrazine under laboratory conditions. Pathway and sensitivity analysis during this phase of the project provide insight into the chemical processes underlying the decomposition of hydrazine that can guide experimental design and modeling efforts for the more complex system which includes the blow-by species.

A detailed chemical kinetic mechanism for the gas-phase decomposition of hydrazine has been developed and tested. The mechanism consists of twelve chemical species participating in 50 reactions, using recent, critically reviewed rate expressions for many of the reactions.¹⁸ Thermodynamic data more recent than that found in the JANNAF

thermodynamic database¹⁹ has been identified for some of the species.

Previously, several experimental studies of the thermal decomposition of hydrazine had been identified in the literature.^{19 to 25} A thorough, critical review of these studies uncovered flaws in some of them that precluded their use as a measure of the validity of the proposed mechanism. The data from two of the papers was retained for use in validating the mechanism over a fairly broad temperature range.

Chemical kinetic modeling using the mechanism developed for this project was performed with the SENKIN (v. 3.0) and CHEMKIN-II mechanism interpreter (v. 3.6) package of software developed at Sandia.^{26, 27} This software package was slightly modified at the Army Research Laboratory and post-processing codes developed there were used to analyze the binary output of the SENKIN code.²⁸

The mechanism has performed quite well as a predictor of hydrazine decomposition when compared to the available data. A complete description of the chemical mechanism for hydrazine decomposition and its behavior under a variety of temperature and pressure conditions will be presented elsewhere.²⁸ It is highly recommended that additional experimental research be performed to provide a more complete set of data for validation of the mechanism. Of particular importance are studies utilizing helium as the bath gas, since this is the ullage gas in the fuel systems.

Advanced Pyrovalve Design

In the interest of safe and reliable valves for future spacecraft, research into advanced pyrovalve technology was initiated in FY98. Initial design criteria included mass reductions, low blow-by, low particulate release, lower pyro-shock, and the capability to be recycled (for some applications).

Research in FY98 and FY99 yielded the fabrication of a new ram, using an advanced sealing technology, and a clone of the ram from the in. Conax valve (used as a basis for comparison). These rams were fabricated in conjunction with a new sleeve that was retrofitted to the older in. Ti 1468-4 PVS housing. The configuration used one concentrically-mounted NSI (in the same fashion as the booster assembly on the in. Conax valve) and no shear fitting, because the tests involving it were primarily focused on the seal at the ram/sleeve interface.

June 1999 held the start of the advanced PVS blow-by testing. This testing of the new ram/sleeve combination revealed that the goal of zero blow-by favored an alternative design. By May 2000, computer aided design efforts began to include work done on Pro/Engineer version 20.0.³⁰ All of the

advanced PVS components were modeled and assembled in such a fashion that gave itself to efficient finite-element analysis studies performed on Pro/Mechanica version 20.0.³¹

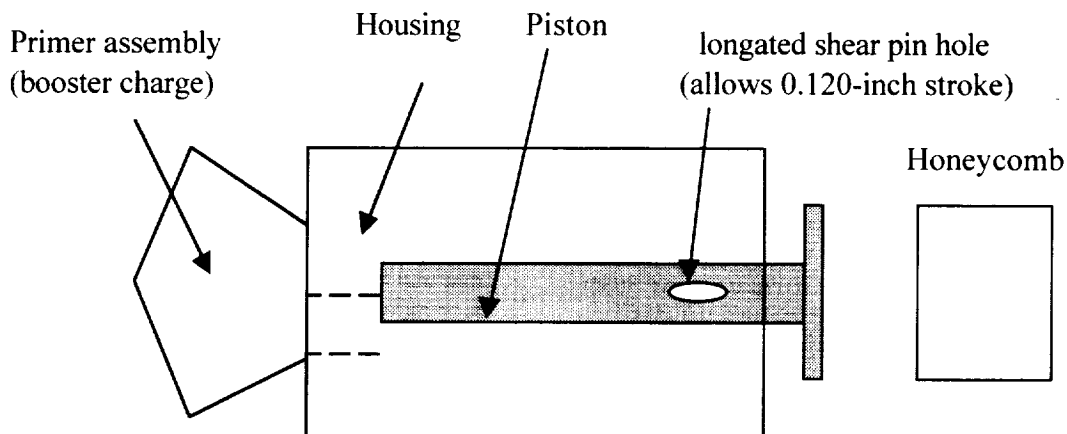
Pro/Mechanica provided a means of modeling the effects of pressure due to the applied pyrotechnic charge on the sleeve and the ram/sleeve sealing interface at different positions. This contributed greatly to insight on what happens to the sleeve during valve actuation. It is this kind of modeling that will be used to finalize alternative designs for the zero blow-by ram.

WSTF PYROVALVE HANDBOOK DEVELOPMENT

Significant data have been and will continue to be generated through various spacecraft propulsion projects involving the use of pyrotechnically operated valves (Pyrovalves). These data need to be fully analyzed, interpreted, summarized, associated, and formatted so they can be made available for spacecraft propulsion system design involving pyrovalves and used to specify test procedures in the evaluation and qualification of these systems. A Pyrovalve Handbook is being developed at the NASA White Sands Test Facility (WSTF) to meet these needs. The current status of this effort that is in the first development stage is outlined in detail in a separate paper.²

The handbook is an applications handbook being formulated under the sponsorship of the NASA Technical Standards Program and incorporating recommended pyrovalve-testing techniques under the sponsorship of the NASA Safety and Risk Management Program. The ultimate goal is to have a shortened version of the handbook adopted as a voluntary standard under the guidance of the AIAA Energetic Components and Systems Technical Committee.

The Air Force Space and Missile Systems Center has recently supported an effort to upgrade design, manufacture, and performance verification criteria of components and systems that contain or are operated by explosive materials. However, pyrovalve applications and tests are not addressed in any depth. The new document is MIL-HDBK-83578, Criteria for Explosive Systems and Devices Used on Space Vehicles. Following release of this document, specifications DOD-E-83578 and standard MIL-STD-1576 are to be cancelled by the Department of Defense (DOD). Additionally, the International Standards Organization (ISO) Technical Committee 20, Subcommittee 14, Working Group 1 (TC20/SC14/WG1) is currently converting the new Air Force handbook into ISO-14304-1 under the



same name. The DOD/ISO Working Group project leader and numerous others, including the AIAA Energetic Components and Systems Technical Committee, enthusiastically endorse the concept of developing a separate Pyrovalve Handbook and including it in the DOD/ISO documents as an Appendix. It is envisioned that a shortened version of the handbook could be adopted as a voluntary consensus standard under the guidance of the AIAA and, in an even more restrictive format, included as part of the ISO standard. It is felt that NASA's spacecraft interests will be served and the Office of Management and Budget (OMB Circular A-119) policy, directing a move to voluntary standards, will be met.

CONCLUSIONS

Significant progress has been made toward meeting the MOCATP objectives since the WSTF program organizational meeting conducted August 23 and 24, 1995. Some of the accomplishments are:

- An extensive capability for testing pyrovalves and pyrotechnically actuated devices has been provided for NASA and industry programs.
- A significant amount of data has been provided from testing and relative hazard levels associated with various pyrovalves, and propellant combinations have been characterized.
- An alternative low blow-by pyrovalve and other corrective actions have been presented.
- Advanced pyrovalve technology development is underway to help meet future spacecraft needs, and
- NDE techniques have been developed and are available for users of O-ring type pyrovalves.

Testing and analysis will continue, leading to documentation of data and findings in a pyrovalve applications handbook.

FUTURE TESTING AND MODELING

Future WSTF Blow-by Testing. Several additional blow-by tests are planned. A $\frac{1}{8}$ -in. Conax valve will be prepared for VISAR testing and will be fully evacuated to remove the air. This valve has been interfaced to the VISAR system using an extension allowing the ram velocity rather than the shear section to be tracked. The valve has also been modified to allow the pressure above the ram to be monitored during valve actuation rod (see the 1999 status paper for details of both Conax modifications²). Funding permitting, several additional OEA valves will also be tested to provide blow-by data for the Pyrovalve Testing and Applications Handbook.

Future Functional Evaluations. The LaRC weight drop test has been applied to one Conax $\frac{3}{8}$ -in. to determine the energy required to operate the valve. To determine energy available to operate the valve, a Pyrovalve Simulator is being developed. This test apparatus, as shown in Figure 10, will easily simulate the pyrovalve interface to the primer assembly/booster charge. The simulator will utilize a steel housing and piston, duplicating the diameter of the pyrovalve ram, and will place the piston at the same initial position as the ram in the valve simulated. However, duplicating the shear force and energy will require further evaluations. A third piston/cylinder test rig will be employed in further weight drop tests to determine the shape and shear area necessary for an inexpensive *shear pin* to duplicate the force/time history and energy

Figure 10. Pyrovalve mockup to measure energy delivered by primer assembly.

consumption characteristics within the valve. Once that *shear pin*" configuration is established, it will be installed through the piston and housing of the test fixture. The elliptical shear-pin hole, shown in Figure 10, will allow the piston to stroke the same distance the pyrovalve rams strokes before engaging the shear section. After the shear pin has failed, the piston will continue to stroke until it reaches the point of *bottoming* in the valve. A calibrated honeycomb cube will be positioned at that site to measure the remaining energy in the piston. The amount of honeycomb crush, multiplied by the honeycomb strength, yields energy in inch-pounds. This value represents the amount of energy that is in excess to that required to function the valve, or the functional margin.

Future N-ray Defect Detection. Additional work using flight type pyrovalves is planned to enhance resolution of O-rings inside CRES material. Additional plans are in place to evaluate the improved NCT capability now available at the McClelland Nuclear Radiation Center. A higher-resolution imaging array has been added since our FY99 evaluation of defects in O-rings inside Ti material. Neutron radiographs of several more CRES pyrovalves and/or PVS assemblies are also planned. These will attempt to enhance the resolution of prescribed inflicted damage on O-rings obscured by CRES bodies. The goal of this additional testing is to extend to CRES pyrovalves the excellent defect-detection resolution demonstrated for Ti pyrovalves and simulators.

Future Dynamic Housing Diameter Measurement. An initiative was also undertaken to help determine why new interference rams as used in Conax valves could have the observed slight amount of blow-by. It was theorized that cylinder-bore expansion due to the shock and high pyrotechnic driving pressure may cause the interference fit to actually form a slight clearance during the fraction of a millisecond that the pyrotechnic reacts. To investigate this, an extensive search was instigated for extremely fast displacement sensors to measure the time behavior of the diameter of a pyrovalve cylinder during its explosive actuation. Technologies considered included inductive, eddy current, laser triangulation, contact LVDT, laser interferometric, optical fiber, and laser light-curtain. Among these technologies, only the laser interferometric and the optical fiber ones had commercial implementations that could be supplied with the required 500 kHz response.

The laser interferometric technology, unfortunately, was far too expensive to be practical for this application, although its frequency response was

higher than any alternative. The optical fiber displacement sensor was available with a 500 kHz response modification, and its implementations were more cost effective for this application.

The laser light-curtain had no commercial implementation that was fast enough for this application, but the Nondestructive Testing group at LaRC has implemented a version expected to exceed 100 kHz response. Both a commercial version of the optical fiber technology and our implementation of the LaRC version of the laser light-curtain technology will be evaluated for the non-contact diameter measurement of a pyrovalve cylinder during normal actuation.

Also, some simple contact sensors will be compared to the commercial non-contact versions. A polymer pressure sensor has already been clamped to the outside of the pyrovalve cylinder for a few of the Conax valve firings. Preliminary data indicated adequate frequency response, but the initial mounting technique seemed to mix radial and circumferential response for the sensor. The response suggested an initial expansion during the pressure phase, followed by a large oscillation about the time the ram hit the shear cap, and then a somewhat smaller oscillation about the time the ram hits its stop. The quantitative relationship of this pressure response to a displacement was, however, not evident.

Future Ultrasonic O-ring NDE. Preliminary conventional ultrasonic images are now in progress. Their features will be compared to those of the other technologies considered in this investigation. The initial test article for this portion of the investigation is a Ti PVS sleeve/ram assembly with various configurations of O-ring damage simulation. Rotational C-scans are being performed through the outside cylinder wall of the PVS adjacent to the location of the interior O-rings.

Future Chemical Kinetics Modeling. Additional modeling work will focus on the development of a mechanism including the blow-by species from the pyrovalves and an analysis resulting in the identification of key reactions likely to initiate (or inhibit) thermal runaway in the more complex system. Adding the blow-by gas chemistry into the model will result in a substantially larger mechanism. Inclusion of the blow-by species and their reactions into the model are critical to understanding the initiation of the destruction of a liquid hydrazine fuel system; however, the importance of understanding the decomposition of hydrazine itself cannot be overlooked. Any reactive blow-by species introduced into the fuel system will be a very minor and localized constituent (compared to the fuel system as a whole) that would be quickly

consumed in their reactions with hydrazine. Once the process leading to thermal runaway has been started, it is the decomposition chemistry of hydrazine itself that must be understood.

ACKNOWLEDGMENT

Several people and organizations have made this paper possible. In addition to the authors, contributors included the MOCATP Manager, Dr. Steve Schneider from the NASA Lewis Research Center and the WSTF MOCATP test team. Personnel contributing data included the WSTF Honeywell Hydrazine Sensitivity Test Project Leader, Kurt Rathgeber, and WSTF Propellant Test Projects Group Leader, Steven Woods. Additionally, the propellant related projects have been conducted under the sponsorship of the NASA Safety and Risk Management Division, where the direct support and interest of Claude Smith and Wayne Frazier have made the projects possible. The O-ring NDE project was made possible by the NASA NDE Working Group, and the blow-by testing was made possible the NASA Metrology Working Group. Advanced pyrovalve development is being sponsored as a JSC Center Director Discretionary Funds Project.

REFERENCES

1. Saulsberry, R., Julien, H. L., Hart, M., Ramirez, J., and Smith, W. "Mars Observer Propulsion and Pyrotechnic Corrective Actions Test Program Review - 1999." 35th *AIAA/ASME/SAE/ASEE Joint Propulsion Conference and Exhibit*, AIAA # 99-2305, Los Angeles, CA, June 20-23, 1999.
2. Julien, H., Hart M. B., Smith W.C., and Saulsberry R. "Status of WSTF Pyrovalve Handbook Development in Year 2000." AIAA Paper 2000-3514, presented at the 36th *AIAA/ASE/SAE/ASEE Joint Propulsion Conference and Exhibit*, Huntsville, AL, July 16-19, 2000.
3. Saulsberry, R. *Mars Observer Propulsion and Pyrotechnics Corrective Actions: Propulsion System Test Program (MOCATP)*. TP-WSTF-854, NASA Johnson Space Center White Sands Test Facility, Las Cruces, NM, December 19, 1995.
4. Saulsberry, R., Julien, H. L., Woods, S. S., Maes, M., and Livingston, R. "Mars Observer Propulsion and Pyrotechnic Corrective Actions Test Program Review - 1998." 34th *AIAA/ASME/SAE/ASEE Joint Propulsion Conference and Exhibit*, AIAA 98-3912, Cleveland, OH, July 13-15, 1998.
5. Fleming, K. J., Tarbell, W. W., and Saulsberry, R. L. "NASA Pyrovalve RAM Velocity Measurements." 32nd *AIAA/ASME/SAE/ASEE Joint Propulsion Conference and Exhibit*. Lake Buena Vista, FL, July 1-3, 1996.
6. Hart, M., Saulsberry, R. L., Abney, K., Maes, M., and Liming, S. "The Application of VISAR During Pyrovalves Blow-by Analysis." 34th *AIAA/ASME/SAE/ASEE Joint Propulsion Conference and Exhibit*, AIAA 98-3914, Cleveland, OH, July 13-15, 1998.
7. Saulsberry, R. L., Abney, K., Hart, M., Rathgeber, K. A., Liming, S., and Hawkins, B. "Evaluation of Low Blow-by Alternative Pyrovalves: Hydrazine Reactivity and Blow-by Measurement." 34th *AIAA/ASME/SAE/ASEE Joint Propulsion Conference and Exhibit*, AIAA 98-3916, Cleveland, OH, July 13-15, 1998.
8. Rathgeber, K. A., Julien, H. L., and Saulsberry, R. L. "Sensitivity of Monomethylhydrazine (MMH) in Pyrovalves." 34th *AIAA/ASME/SAE/ASEE Joint Propulsion Conference and Exhibit*, AIAA 98-3913, Cleveland, OH, July 13-15, 1998.
9. Barragan, M., Woods, S. S., Julien, H. L., Wilson, D. B., and Saulsberry, R. L. "A Multiphase Equation of State for Hydrazine and Monomethylhydrazine." 35th *AIAA/ASME/SAE/ASEE Joint Propulsion Conference and Exhibit*, AIAA 99-2418, Los Angeles, CA, June 20-23, 1999.
10. Julien, H. L., Woods, S. S., Rathgeber, K. A., Forsyth, B., Reynolds, M., Barragan, M., Saulsberry, R. L., and Meagher, N. "Explosive Events Initiated by Pyrovalves." 35th *AIAA/ASME/SAE/ASEE Joint Propulsion Conference and Exhibit*, AIAA 99-2418, Los Angeles, CA, June 20-23, 1999.
11. Gazze, C. E. "The overtical Isp Program Documentation." Propulsion Group Report, Edwards AFB, August 1990
12. Bement, Laurence J.: Functional Performance of Pyrovalves. *Journal of Spacecraft and Rockets*. Vol. 34. No. 3, May-June 1997.
13. Bement, Laurence J. and Multhaup, Herbert A.: Determining Functional Reliability of Pyrotechnic Mechanical Devices. *AIAA Journal*, Vol. 37, No. 3, March 1999.
14. Garcia, B. O., Chavez, D. J., and Linley, L. J. *Detonability Study of Liquid Hydrazine*. Unpublished draft, NASA Johnson Space Center White Sands Test Facility, Las Cruces, NM, 1993.

15. Garcia, B. O. *The Shock Hugoniot of Liquid Hydrazine in the Pressure Range 3.1 to 21.4 GPa*. Thesis for a Master of Science of Engineering Mechanics, New Mexico Tech., Socorro, NM, April 27, 1996.
16. Barragan, M., Woods, S. S., and Wilson, D. B. "An Equation of State for Hydrazine and Monomethylhydrazine, Its Validation and Use for Calculation of Thermodynamic Properties." *1998 JANNAF Propellant Development and Characterization Subcommittee and Safety and Environmental Protection Subcommittee Joint Meeting*, Houston, TX, April 20-24, 1998.
17. Barragan, M., Julien, H. L., Woods, S., Wilson, D. B., and Saulsberry, R. "Isentropic Compression of Mixtures of Fuels and Inert Gasses." AIAA Paper 2000-3516, presented at the 36th AIAA/ASE/SAE/ASEE Joint Propulsion Conference and Exhibit, Huntsville, AL, July 26-19, 2000.
18. Dean, A. M. and Bozzelli, J. W. Combustion Chemistry of Nitrogen, in *Gas-Phase Combustion Chemistry*; Gardiner, W. C., Jr., Ed.; Springer-Verlag: New York, 2000; Chapter 2.
19. Kee, R. J., Rupley, F. M., and Miller, J. A. (Sandia Thermodynamic Database Reference) Technical Report SAND87-8215, Sandia National Laboratories, Albuquerque, NM, April 1987.
20. Michel, K. W., and Wagner, H. G., "The Pyrolysis and Oxidation of Hydrazine behind Shock Waves." *Tenth Symposium (International) on Combustion*, The Combustion Institute, 1965, pp. 353-364.
21. Eberstein, I. J., and Glassman, I. "The Gas-Phase Decomposition of Hydrazine and Its Methyl Derivatives." *Tenth Symposium (International) on Combustion*, The Combustion Institute, 1965, pp. 365-374.
22. Moberly, W. H. "Shock Tube Study of Hydrazine Decomposition." *Journal of Physical Chemistry*, 1962, 66, pp. 366-368.
23. Halat-Augier, C., Dupre, G., and Paillard, C. E. "Thermal Decomposition of Gaseous Hydrazine behind a Reflected Shock Wave." *Proceedings of the 20th International Symposium on Shock Waves*, Vol. II, Pasadena, CA, July 1995, pp. 893-898.
24. Diesen, R. W. "Mass Spectral Studies of Kinetics behind Shock Waves. II. Thermal Decomposition of Hydrazine." *Journal of Chemical Physics*, 1963, 39, pp. 2121-2128.
25. McHale, E. T., Knox, B. E., and Palmer, H. B. "Determination of the Decomposition Kinetics of Hydrazine using a Single-Pulse Shock Tube." *Tenth Symposium (International) on Combustion*, The Combustion Institute, 1965, pp. 341-351.
26. Kee, R. J., Rupley, F. M., and Miller, J. A. (Sandia Chemkin-II code reference) Technical Report SAND89-8009, Sandia National Laboratories, Albuquerque, NM, September 1989.
27. Lutz, A. E., Kee, R. J., and Miller, J. A. (Sandia Senkin code reference) Technical Report SAND87-8248, Sandia National Laboratories, Albuquerque, NM, October 1988.
28. Anderson, W. R., Haga, S. W., Nuzman, J. F., Kotlar, A. M. SREAD computer code. U.S. Army Research Laboratory, developed continuously 1990-present. There is no written documentation, but the codes are available for dissemination.
29. Meagher, N. E., Bates, K. R., and Smith, S. G. *To be published*.
30. "Pro/ENGINEER Version 20.0." Waltham, MA. Parametric Technology Corporation, 1998.
31. "Pro/MECHANICA Version 20.0." Waltham, MA. Parametric Technology Corporation, 1998.



